

Development of Miniature, High Frequency Pulse Tube Cryocoolers*

Ray Radebaugh,¹ Isaac Garaway,¹ and Alexander M. Vepruk²

¹National Institute of Standards and Technology, Boulder, Colorado 80303 USA

²Ricor, Cryogenic and Vacuum Systems, En Harod, 18960, Israel

ABSTRACT

Because acoustic power density is proportional to frequency, the size of pulse tube cryocoolers for a given refrigeration power can be reduced by operating them at higher frequencies. A frequency of about 60 Hz had been considered the maximum frequency that could be used while maintaining high efficiency. Recently, we have shown through modeling that by decreasing the volume and hydraulic diameter of the regenerator and increasing the average pressure, it is possible to maintain high efficiency even for frequencies of several hundred hertz. Subsequent experimental results have demonstrated high efficiencies for frequencies of 100 to 140 Hz. The very high power density achieved at higher pressures and higher frequencies leads to very short cooldown times and very compact devices. The use of even higher frequencies requires the development of special compressors designed for such conditions and the development of regenerator matrices with hydraulic diameters less than about 30 μm . To demonstrate the advantages of higher frequency operation, we discuss here the development of a miniature pulse tube cryocooler designed to operate at 80 K with a frequency of 150 Hz and an average pressure of 5.0 MPa. The regenerator diameter and length are 4.4 mm and 27 mm, respectively. The lowest temperature achieved to date has been 97 K, but a net refrigeration power of 530 mW was achieved at 120 K. Acoustic mismatches with existing compressors significantly limit the efficiency, but necessary modifications to improve the acoustic impedance match between the compressor and the cold head are discussed briefly.

Keywords: Cryocoolers, cryogenics, detectors, high frequency, high power density, miniature, pulse tubes, refrigerators, review, sensors, Stirling

1. INTRODUCTION

A clear gap exists between the rapid development and miniaturization of low-temperature sensor applications and the availability of applicable miniaturized cryocoolers. Many of these applications are optical and electronic based technologies that by nature require only a relatively small heat lift (typically 1 W or less) but do need short cooldown times. As a result of the inherent difficulties which have hampered the development of miniature closed loop JT cryocoolers, which were originally thought to be best suited for these applications, there has been a growing interest in miniaturizing regenerative devices such as the pulse tube cryocooler. A regenerative cycle operates with a relatively small cyclic pressure wave oscillating around a large average fill pressure, rather than the constant large pressure ratio needed in a recuperative (JT) cycle. The guiding principle in the transition to regenerative cycles is that the compressor necessary in regenerative cycles may be realized on considerably smaller scales if the cycle frequency and fill pressure are increased to deliver the same PV power with much smaller piston swept volume. Much of the initial foundational theoretical work to this effect was to set forth the basic operating parameters and characteristics of such miniature high frequency pulse tubes. Peterson et al. [1] and others [2] began this effort in the mid 1990's by trying to establish a theoretical lower size limit in general to regenerative cryocooler miniaturization. Other work, more specific to actual cryocooler design, such as Radebaugh [3, 4], focused on heat transfer phenomena in small dimensions and at higher frequency operation. Here issues of cycle frequency with respect to regenerator gas volume and thermal penetration into the heat transfer media were studied so as to establish the necessary operating parameters and regenerator geometries necessary to design viable high frequency miniature cryocoolers.

* Contribution of NIST, not subject to copyright in the U. S.

Attempts to experimentally develop high frequency miniature pulse tube cryocoolers [5-7] have been met with many difficulties, and it was only recently that a high frequency miniature cryocooler, built at NIST, was able to successfully reach temperatures below 100 K [8]. In that work, a miniature pulse tube cryocooler designed to operate at a frequency of 120 Hz and an average pressure of 3.5 MPa achieved a no-load temperature of 50 K and provided 3.35 W of net refrigeration power at 80 K. Even with large cold-end flanges, the cooldown time to 80 K was only 5.5 minutes. While this cryocooler, with a regenerator length of only 30 mm, did fulfill its stated purpose and showed how such a miniaturized cold head could perform at higher operating frequencies, it was driven by a relatively large (in comparison to the cold-head dimensions) compressor (~ 5 liters in volume) that was limited to much lower pressures than what are optimal for such miniature systems. Though the system efficiency with respect to input PV power was above 16% of Carnot, the input electrical power was quite high (about 275 W) because the linear compressor was operating far from its design resonance conditions. More recently Petach *et al.* [9] described a miniature high frequency coaxial cryocooler developed for space applications that provided 1.3 W of cooling at 80 K at an efficiency of 8.8% of Carnot when operating at 100 Hz. They also tested the cooler at frequencies up to 144 Hz, but with reduced efficiency because the compressor was running off resonance at these higher frequencies.

To further establish the viability of using high pressure and high frequency pulse tube cold heads as a means of miniaturizing the entire cryocooler, a subsequent 150 Hz pulse tube cold head was designed [10]. The regenerator had dimensions of 4.4 mm inside diameter and 27 mm length, and was filled with #635 mesh stainless steel screen. A net refrigeration power of about 0.5 W at 80 K was numerically predicted for this miniature pulse tube cryocooler, given a pressure ratio of 1.3 at the cold end. A miniature linear compressor (Ricor K527) capable of operating at frequencies up to 200 Hz and at elevated pressures of up to 5.0 MPa and having an overall volume of ~ 100 cm³ was employed to drive this pulse tube cold finger. It has a peak-to-peak swept volume of 0.567 cm³. The initial testing results showed that while the pulse tube did deliver rapid cool-down to temperatures below 100 K (~97 K), the inability of the miniature compressor to provide the modeled 1.3 pressure ratio prevented it from reaching its design point of net cooling at 80 K. Due to this inconsistency between the model and the realities of needing to work with a "real" miniature compressor, this pulse tube cryocooler underwent a process of optimization in light of the attached miniature compressor and thus lower pressure ratios. This study highlights the need to further establish our understanding of miniature, high frequency, regenerative cryocoolers, not only as a collection of independent subcomponents, but as one single working unit. This paper describes the process of diagnostics on the pulse tube cryocooler, the optimization schemes, and the resulting improvements. Suggested changes to compressor parameters are given that would lead to a compressor resonance at higher pressure ratios. Such a compressor and pulse tube cold finger would have a very high power density, which permits further miniaturization.

2. CRYOCOOLER THERMODYNAMICS

2.1 Effect of Frequency on Compressor Size

The size and mass of Stirling and Stirling-type pulse tube cryocoolers are dominated by the size and mass of the pressure oscillator (compressor). The acoustic or PV power delivered by the pressure oscillator is given by

$$\dot{W}_{PV} = \frac{1}{2} P_1 \dot{V}_1 \cos \theta, \quad (1)$$

where P_1 and \dot{V}_1 are the amplitudes of the sinusoidal pressure and the volume flow, as given by

$$P = P_0 + P_1 \cos \omega t \quad (2)$$

and

$$\dot{V} = \dot{V}_1 \cos(\omega t + \theta). \quad (3)$$

The term P_0 is the average pressure, ω is the angular frequency, and θ is the phase by which the volume flow leads the pressure. The sign convention used here is that the volume flow is positive for flow leaving the pressure oscillator. The volume flow amplitude is related to the instantaneous volume amplitude V_1 in the pressure oscillator by

$$\dot{V}_1 = 2\pi f V_1. \quad (4)$$

The PV power is then given by

$$\dot{W}_{PV} = \pi f V_1 P_0 \left(\frac{P_1}{P_0} \right) \cos \theta, \quad (5)$$

where f is the frequency. The term in parentheses is the relative pressure amplitude. From this equation we see that by increasing the frequency the volume amplitude V_1 can be reduced for the same PV power. An increase in the average pressure also allows for a decrease in the volume amplitude. The total swept volume of the pressure oscillator is $V_{co} = 2V_1$. Similarly the swept volume of the displacer at the cold end of a Stirling cryocooler or the volume of the pulse tube in a pulse tube cryocooler can be decreased for the same gross refrigeration power (net refrigeration plus losses) by increasing the frequency and/or the average pressure.

The total volume of a compressor or pressure oscillator is much larger than that of the swept volume, but there will be some correlation between the two. The total volume is typically about 100 times the swept volume, at least for 60 Hz compressors. The total compressor volume is usually proportional to the volume of the linear motor. We discuss some scaling laws for the linear motor in a later section. We recognize that the reduction factor for the entire compressor will not be as great as that of the swept volume, but a significant reduction of the compressor would be possible with higher operating frequencies. Unfortunately, simply increasing frequency in a regenerative cryocooler without making changes in other parameters leads to very low efficiencies.

2.2 Maintaining High Efficiency at High Frequencies

Figure 1 shows a phasor representation for mass conservation within the regenerator of a Stirling cryocooler, where the dynamic pressure at the cold end is along the real axis. Because of the gas volume in the regenerator, the conservation of mass requires that the flow at the warm end will lead the flow at the cold end and is given by

$$\dot{m}_h = \dot{m}_c + \frac{\dot{P} V_{rg}}{RT_r}, \quad (6)$$

where the bold variables represent time varying or phasor quantities, \dot{m}_c is the flow rate at the cold end, V_{rg} is the gas volume in the regenerator, R is the gas constant per unit mass, T_r is the mean temperature of the regenerator, and \dot{P} is the rate of change of pressure in the regenerator, given by

$$\dot{P} = i2\pi f P, \quad (7)$$

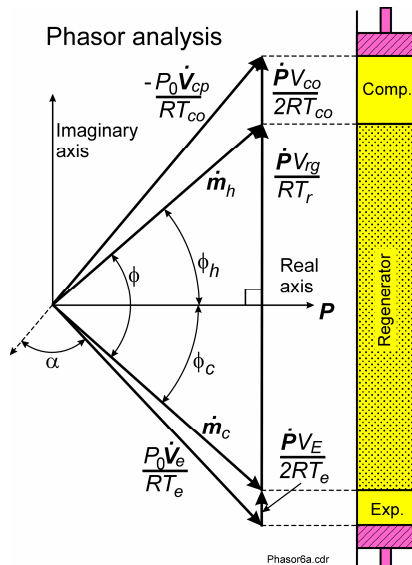


Figure 1. Phasor diagram for mass conservation in a Stirling cryocooler.

where i is the imaginary unit and P is the dynamic pressure. This phasor leads the pressure by 90° , as indicated by the vertical phasor along the imaginary axis in Figure 1. The second term on the right-hand side of Equation (6) represents the rate of change of gas mass within the regenerator.

The optimum phase relationship between flow and pressure is that in which the flow at the regenerator midpoint is nearly in phase with the pressure. With such a phase relationship the magnitude of flow at each end is minimized for a given acoustic power flow through the regenerator [10]. Losses in the regenerator are proportional to the flow magnitude. Typically the flow at the cold end will lag the pressure by about 30° , whereas at the warm end the flow will lead the pressure by about 30° . Such a phase relationship is easily achieved in a Stirling refrigerator by selecting the appropriate swept volume and phase for the displacer. The same phasor diagram would apply to a pulse tube cryocooler where the phase of the flow at the cold end would be established by an inertance tube at the warm end of the pulse tube.

According to equation (7), \dot{P} and the vertical phasor in Figure 1 increase with frequency. Thus, at very high frequencies the magnitude of the flow and the swept volume at the warm end become very large for a fixed flow and acoustic power at the cold end. In that case the regenerator loss becomes very high. To keep the vertical phasor (rate of mass change) from increasing significantly as frequency is increased, the regenerator gas volume V_{rg} must be reduced as frequency increases. Our goal is to keep the hot-end phase angle ϕ_h nearly constant as the frequency increases. That goal is satisfied if the ratio of the vertical phasor to the mass flow amplitude is held constant as frequency is increased, as given by

$$\frac{\dot{P}V_{rg}}{\dot{m}_1RT_r} = \frac{2\pi f P_1 V_{rg}}{\dot{m}_1RT_r} = \text{constant.} \quad (8)$$

As the regenerator gas volume is decreased, the heat transfer area must be maintained for a given effectiveness, which requires the hydraulic diameter to be reduced. Other geometrical parameters must also be changed in a manner such that the conduction loss and the pressure drop are kept constant as the volume is decreased. Radebaugh and O’Gallagher [3] used an analytical model to derive the parameters involved in the constant of Equation (8). To maintain losses (conduction, regenerator thermal loss, pressure drop) constant for any change in frequency, they showed that Equation (8) can be given by

$$\frac{\dot{P}V_{rg}}{\dot{m}_1RT_r} \propto \frac{f(1-n_g) \int k_{eff} dT}{n_g P_0 (P_1/P_0)^2} = \text{constant,} \quad (9)$$

where n_g is the porosity and k_{eff} is the effective thermal conductivity between the low and high temperatures. From Equation (9) we see that as frequency is increased, the average pressure or pressure ratio must be increased to maintain a constant value for the expression and to prevent the phase angle for warm-end flow from increasing. We have found from more detailed numerical analyses that it is best to keep the pressure ratio constant and increase the average pressure. A companion equation from reference [3] shows that the optimum hydraulic diameter varies as the inverse of the average pressure and the relative dynamic pressure (relative to the average pressure).

3. OPTIMIZATION PROCEDURE FOR A 150 HZ PULSE TUBE CRYOCOOLER

3.1. Pulse Tube Cryocooler Schematic and Fixed Parameters

In any given systems we are usually faced with some constraints on some of the many parameters associated with a cryocooler system. In this case the compressor provided some limitations, such as a maximum average pressure of 7 MPa and a maximum frequency of 200 Hz. In order to stay closer to the compressor resonant frequency we decided to design for an operating frequency of 150 Hz. From experience with modeling many 60 Hz pulse tube cryocoolers, we decided to use a cold-end pressure ratio of 1.3 to give a fairly high power density and overall efficiency. We found later that such a high pressure ratio was not such a good match to the available compressors. A pulse tube cold head was selected instead of a Stirling cold head to keep the construction simple. A schematic of such a system is shown in Figure 2. The inertance tube shifts the phase between the flow and pressure, although for small systems with low acoustic power the maximum phase shift can be fairly small and significantly less than the optimum. As discussed in the previous section, the hydraulic diameter must decrease as the average pressure is increased to maintain nearly constant efficiency. Presently the finest commercially available screen is #635 mesh, made with stainless steel wire of 20.3 μm diameter and with a porosity of about 0.601. We then decided to use this screen and optimize the other parameters around this constraint. The tube wall for the regenerator was to be stainless steel for ease of manufacture. The effective thermal conductivity of the stainless steel screen was set at 0.13 times the solid conductivity of stainless steel to account for the many layers of mesh [11].

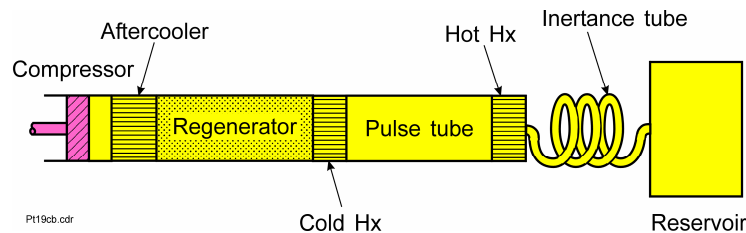


Figure 2. Schematic of a pulse tube cryocooler with an inertance tube for phase shifting.

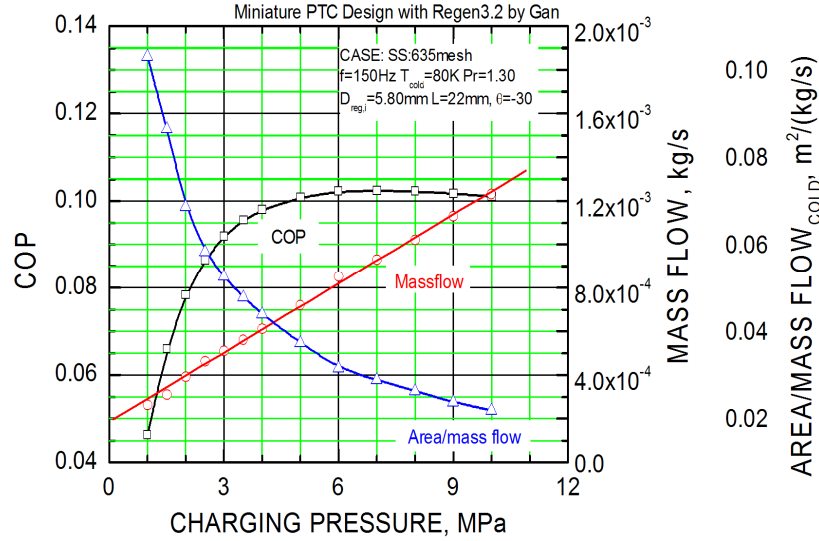


Figure 3. Effect of charging pressure on COP, cold-end mass flow, and specific area.

3.2. Numerical and Analytical Models

The NIST numerical model REGEN3.2 for the analysis of regenerators was used for the optimization of the 150 Hz regenerator [12, 13]. It uses finite differences to model the four conservation equations. One of the boundary conditions is the phase of the cold-end flow with respect to dynamic pressure at the cold end. This program is used to find the maximum coefficient of performance COP for the regenerator by varying several parameters. Usually the cold-end flow is varied for a fixed regenerator diameter and finding the maximum COP. The regenerator COP is given by

$$\text{COP} = \frac{\dot{Q}_{net}}{\langle \dot{W} \rangle_h}, \quad (9)$$

where \dot{Q}_{net} is the net refrigeration power and $\langle \dot{W} \rangle_h$ is the acoustic or PV power at the regenerator hot end. The regenerator COP is plotted as a function of the specific area A_g / \dot{m}_c , where A_g is the gas cross-sectional area and \dot{m}_c is the mass flow rate at the cold end. The results can then be scaled to any size system by varying the area proportional to the flow rate to keep the ratio constant. All other geometrical parameters, such as length and hydraulic diameter remain constant as size is varied in order to keep the COP constant. A separate program based on a transmission line model was used to find the maximum phase shift possible using an inertance tube operating at the conditions required here [14]. The compliance volume associated with the pulse tube leads to about a 30° phase shift between the flow at the two ends of the pulse tube. Thus, to achieve an approximate optimum phase of -30° at the cold end requires the inertance tube to provide a phase shift of -60° (flow lagging pressure). If the inertance tube is replaced with a simple orifice the flow and pressure would be in phase at the pulse tube warm end, but the flow at the cold end would lead pressure by about $+30^\circ$.

3.3. Effect of Average Pressure

A preliminary regenerator optimization was carried out by fixing the regenerator diameter and varying the cold-end flow and the regenerator length to find the maximum COP for a given average pressure. Figure 3, taken from reference [10], shows how the average pressure affects the COP and the optimum A_g / \dot{m}_c . From this figure we see that an average pressure of 5.0 MPa is near the optimum value for #635 mesh screen and a pressure ratio P_{max}/P_{min} at the cold end of 1.3. Further optimization was then carried out using an average pressure of 5.0 MPa and a cold-end pressure ratio of 1.3.

3.4 Optimum Diameter and Length

Figure 4 shows how the maximum COP occurs at a regenerator length of about 27 mm and a specific gas area of $0.022 \text{ m}^2 \cdot \text{s}/\text{kg}$. These optimization results are for a phase angle of -30° at the cold end. Figure 5 shows how the COP varies

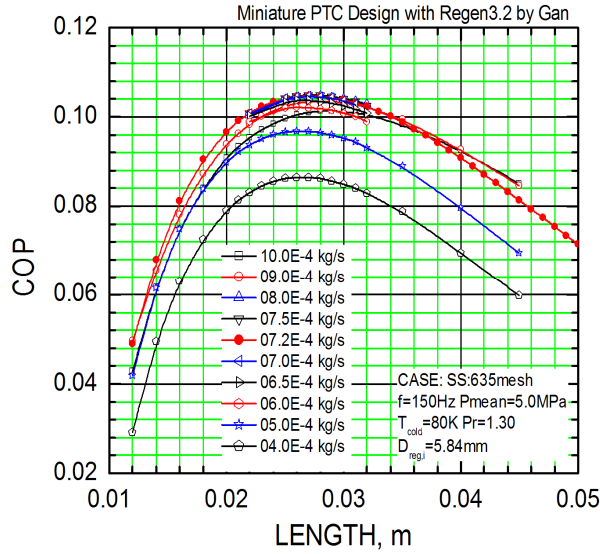


Figure 4. Effect of length on COP for various flow rates.

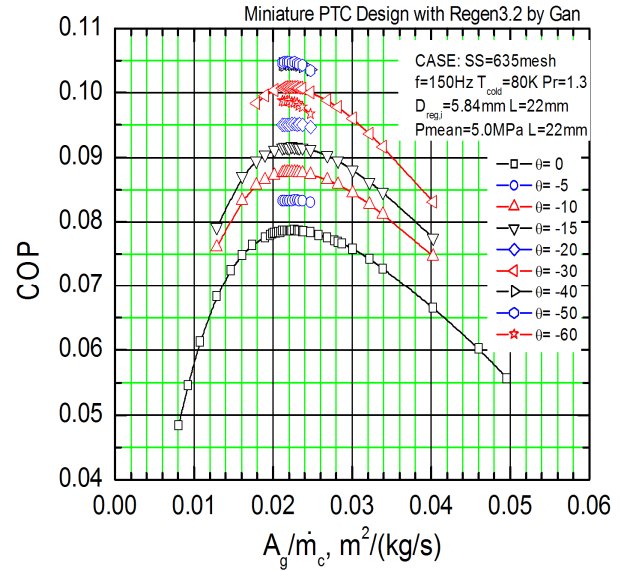


Figure 5. Effect of cold-end flow phase on COP.

with the cold-end phase angle. It also shows that the optimum specific area remains constant for various phase angles. We also found that the optimum length remains nearly constant as the phase angle changes.

3.5 Optimized Design Parameters and Calculated Performance

With the regenerator optimization procedure described above and with the phase angle determined from the inertance tube model, the optimized design parameters were found. Table 1 lists the optimized design parameters for this 150 Hz miniature pulse tube cryocooler. The mass flow amplitude at the cold end was to be 0.37 g/s at a phase angle of 0° with respect to the pressure. With a pressure ratio of 1.3 at the cold end and with 0.8 as the pulse tube effectiveness (ratio of time-averaged enthalpy flow to acoustic power flow), the calculated net refrigeration power was about 1.0 W at 80 K with an input PV power of about 18 W. In order to evaluate and further establish the validity of the design parameters reached by REGEN3.2, the modeling software SAGE by Gedeon Associates was used as a comparative tool. The results from running “SAGE 4.0 Pulse Tube Solver” confirmed that a cryocooler built with these design parameters should be able to achieve cooling at 80 K, but it predicted only about 0.5 W vs. the 1 W predicted by the REGEN3.2

Table 1a. Design operating parameters for miniature, 150 Hz pulse tube cryocooler.

T_c (K)	T_h (K)	Q_{net} (W)	P_0 (MPa)	P_r (cold)	f (Hz)	\dot{m}_c (g/s)	ϕ_c (deg)	\dot{W}_h (W)
80	300	1.0	5.0	1.3	150	0.391	-30	13.5

Table 1b. Optimized design geometry for miniature, 150 Hz pulse tube cryocooler.

	After cooler	Regen.	Cold HX	Pulse Tube	Warm HX	Inertance tube, small	Inertance tube, large	Reservoir 15 cc
Length (mm)	3.3	27.0	2.7	40.4	2.1	23.5	61.0	30
I. D. (mm)	4.63	4.5	2.1	2.1	2.0	0.45	0.80	25
Filling	# 200 Cu	#635 S.S.	#200 Cu	-	#100 Cu	-	-	-

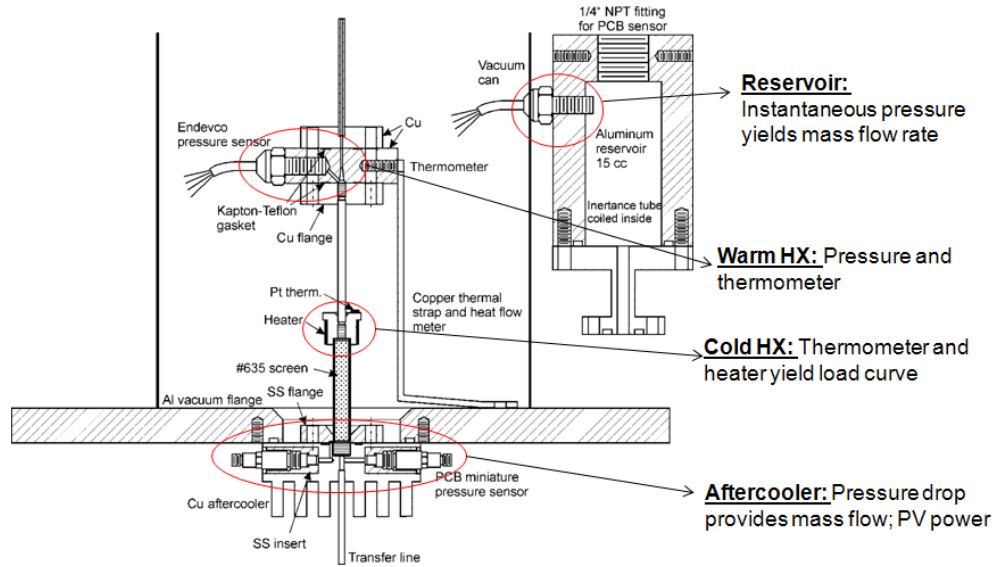


Figure 6. Schematic of inline pulse tube cryocooler with measuring instruments.

model. The discrepancy might be a result of SAGE 4.0 taking into account actual losses within the pulse tube that were not adequately accounted for by using the arbitrary empirical factor of 0.8 for the pulse tube effectiveness in REGEN3.2. A schematic of the optimized 150 Hz miniature pulse tube cryocooler is shown in Figure 6 along with the important measuring devices to characterize the performance of various components.

4. CONSTRUCTION OF 150 HZ PULSE TUBE CRYOCOOLER

The small size of this pulse tube cryocooler coupled with the need to include an adequate amount of sensors to perform testing brought about some design considerations which will be discussed here. The cold head subcomponents were all vacuum brazed together as their small size made the inclusion of “screwable” flanges on each subcomponent quite impossible. As it was, even brazing these small subcomponents together correctly, required designing brazing jigs to keep the parts axially aligned and supported throughout the brazing process. In addition, two supporting bars were mounted within the vacuum can to align the weight of the warm heat exchanger and phase shifting components so that these components would not buckle the thin wall (0.08 mm) of the pulse tube, see Figure 7. This support mechanism was designed to limit any planar movement and yet allow for axial contraction as occurs with cooling. These same supporting rods also double as the conduction cooling path for the warm heat exchanger and reservoir. Other design

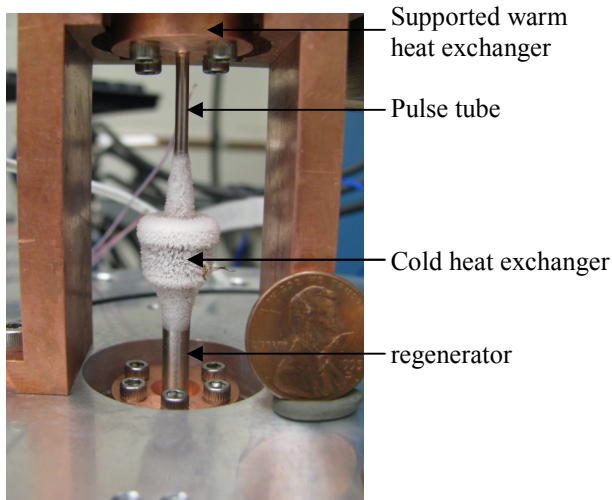


Figure 7. Photograph of cooler.



Figure 8. Photograph of the Ricor K527 compressor used for the initial tests.

considerations include connecting the reservoir to the supporting rod alongside the warm heat exchanger so that all the heat rejected at the warm end of the pulse tube and in the reservoir would need to travel down these same supporting rods to be dissipated on the bottom vacuum plate. This single conduction path provides a means by which the total heat dissipated from the warm end of the pulse tube may be measured. The Ricor K527 compressor (0.567 cm³ swept volume), as shown in Fig. 8, was mounted just below the vacuum plate, relatively close to the aftercooler so as to minimize unnecessary dead volume in the transfer line. The aftercooler was mounted directly onto the outside of the vacuum plate so as to thermally sink it to the much larger thermal mass of the plate and still allow convection cooling from external fans if necessary.

5. EXPERIMENTAL MEASUREMENTS AND RESULTS

5.1 Initial Performance Measurements

The cooler was initially operated with various powers applied to the K527 compressor, and the cold-end temperature was recorded as a function of time. Figure 9 shows these cooldown curves for various pressure ratios at the cold end. The maximum pressure ratio achieved with this compressor was 1.17 as opposed to the 1.3 used in the design. A no-load temperature of 97.5 K was achieved with the pressure ratio of 1.17. Even with this low pressure ratio the cold end reached 100 K in less than 100 s.

The support rods for the warm end of the pulse tube carried the heat rejected at the warm heat exchanger and reservoir. They were turned into a heat flow meter by attaching two thermometers along their length and calibrating the device with a know heat input. The heat flow in these rods is equal to the time-averaged enthalpy flow $\langle \dot{H} \rangle_{pt}$ in the pulse tube, which is related to the pulse tube effectiveness by

$$\eta_{pt} = \frac{\langle \dot{H} \rangle_{pt}}{\langle P\dot{V} \rangle_{pt}}, \quad (10)$$

where $\langle P\dot{V} \rangle_{pt}$ is the acoustic power flow in the pulse tube (from cold to hot). For a perfectly adiabatic process within the pulse tube and no end effects the effectiveness is 1.0. The design calculations used a value of 0.8. To measure the acoustic power in the pulse tube the pressure and flow must be measured at the warm end. The pressure was measured with the pressure transducer mounted on the pulse tube warm end. The flow can only be measured at the entrance to the reservoir by the use of the pressure transducer mounted on it. The flow is related to the time rate of change of the oscillating pressure, which leads the sinusoidal pressure by 90°. The amplitude was determined from the known volume of the reservoir. The inertance tube model was used to make the small correction for the change in flow amplitude (about 14 %) and phase (about 12°) between the reservoir and the pulse tube warm end. Early measurements showed quite low pulse tube effectiveness. Another clue that led us to suspect some form of unstable flow in the pulse tube was the unstable behavior of the cold-end temperature - it never stabilized, but continued to oscillate with large (20 K to 40 K) erratic temperature swings.

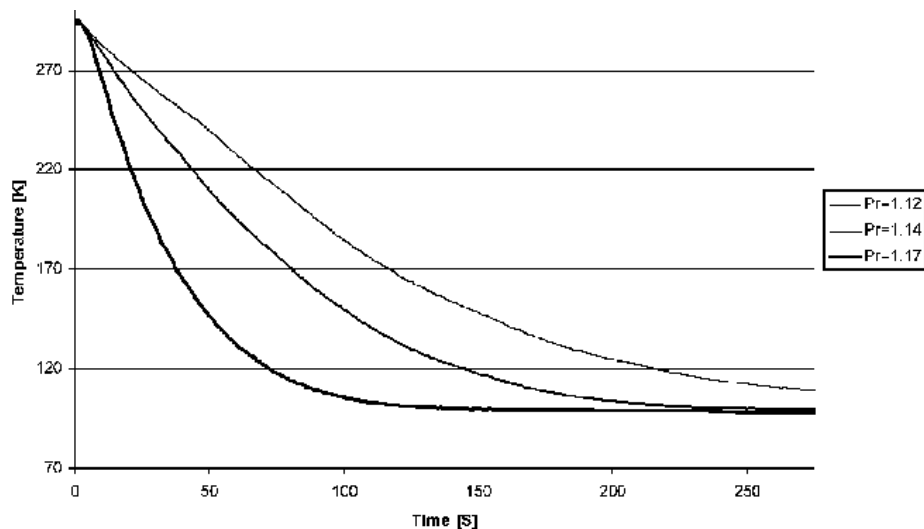


Figure 9. Cooldown curves with various cold-end pressure ratios during initial tests using K527 compressor.

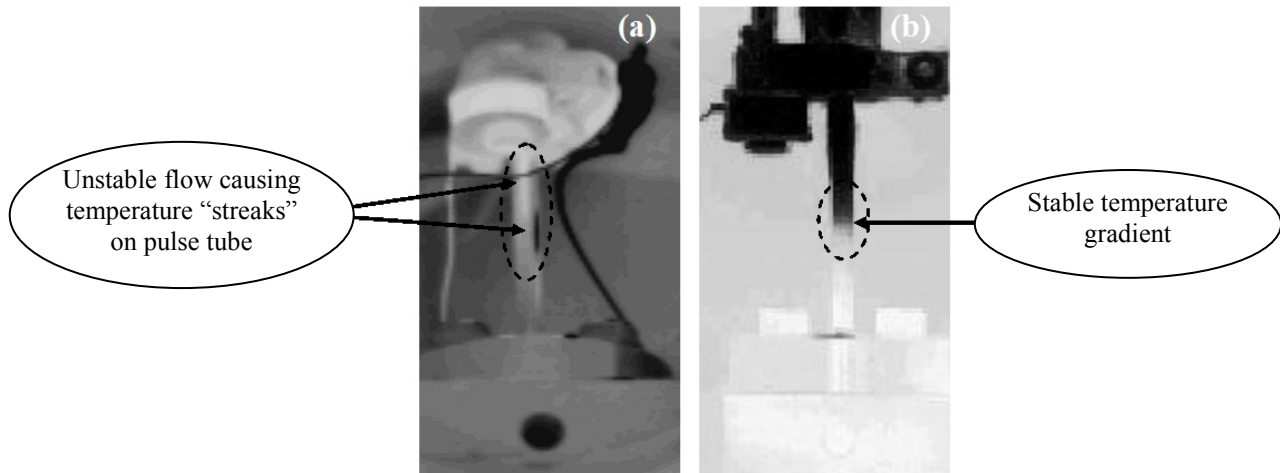


Figure 10. Infrared images of (a) flow instabilities in pulse tube and (b) stable flow after revision.

5.2 Diagnostic Measurements

By using an infrared camera and an appropriately designed infrared germanium window, we were able to film the cold head under operating conditions for temperatures above about 240 K. We were able to determine that the cold heat exchanger temperature instability and the overall poor efficiency of the cryocooler were in fact being caused by flow instabilities in the pulse tube component. Even though the #100 copper mesh, initially used as the heat exchanger medium for the warm heat exchanger, was sufficient with respect to heat transfer, it was too coarse for effective flow straightening at these small dimensions and high frequencies. By replacing the #100 mesh copper stack with a bi-layer stack consisting of ~20 pieces of #200 mesh copper with an additional ~8 pieces of #450 mesh stainless steel (with the steel mesh placed on the end between the copper mesh and the pulse tube opening), we significantly improved the flow behavior. Figure 10 shows two infrared images that provide a comparison between the unstable flow washing through the pulse tube with the initial #100 mesh copper and the stable temperature gradient in the corrected condition with the bi-layer of copper and stainless steel mesh.

5.3 Optimized Performance

The initial measurements on this pulse tube cryocooler were made while using the Ricor K527 compressor to drive the cold head. Because the maximum pressure ratio was limited to 1.17, we decided to use a slightly larger compressor, Ricor K529 (0.785 cm³ swept volume) to obtain a higher pressure ratio. This compressor was able to provide a pressure ratio of 1.20 at the maximum input electrical power of about 70 W. Further optimization of the cryocooler was then carried out, which included varying the diameter and length of the larger diameter inertance tube. The inner diameter was varied at first, and the optimum value was found to be 0.73 mm. The length was then varied, and Figure 11 shows

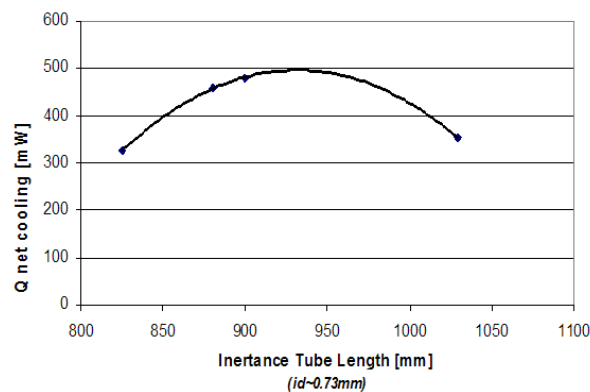


Figure 11. Net refrigeration power as a function of inertance tube length with other parameters kept constant.

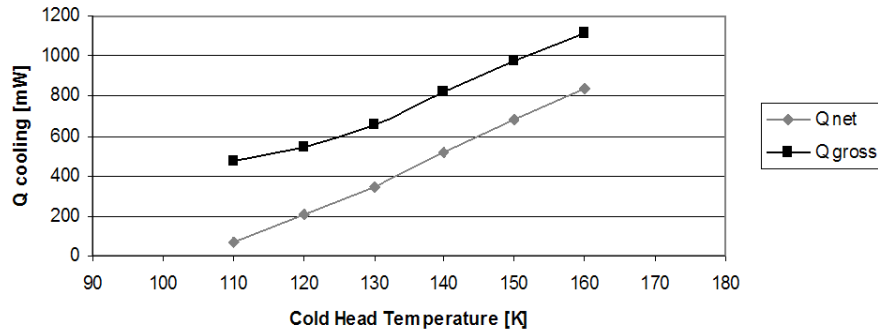


Figure 12. Refrigeration power as a function of cold-end temperature for an input power of 25 W.

that the optimum length should be about 0.93 m to provide maximum refrigeration at 140 K compared with the 0.61 m determined from the modeling. A frequency of 138 Hz was used for these and subsequent measurements because it maximized the cooling. The measured phase shift at the inertance tube entrance provided by this inertance tube was about -50° , which is much higher than the design value of about -30° . The larger phase shift is a result of the pressure ratio being much less than the design value of 1.3. The optimized load curve for an electrical power input of 25 W is shown in Figure 12. The net refrigeration power and the system COP as a function of input power are shown in Figure 13 for a cold-end temperature of 140 K. The system is fairly efficient for low powers (about 5 % of Carnot), but at higher power levels the acoustic mismatch between the cold head and the compressor leads to low COP and efficiency.

6. ACOUSTIC IMPEDANCE MATCH WITH LINEAR COMPRESSOR

The significant parameters of the Ricor K527 and K529 compressors are given in Table 2. With such parameters we can calculate the intrinsic efficiency of a compressor whenever it is operating at resonance conditions. If we know the operating conditions and the acoustic impedance of the attached cold head, we can also calculate the compressor efficiency when it is operating away from resonance conditions. To understand resonance conditions we show in Figure 14 the generalized force balance on the piston in the complex frequency domain [15]. For resonance and maximum compressor efficiency the motor force phasor should be in phase with the velocity (along the imaginary axis or 90° with respect to the real axis). The force provided by the current flow in the coil must balance the sum of the mechanical spring force, the gas spring force, the damping force, and the inertial force. For this compressor the damping coefficient is not known, but if we assume the damping coefficient, eddy currents, hysteresis, and piston blowby are zero, then Joule heating in the coil becomes the only loss. The maximum swept volume of the K527 compressor is 0.567 cm^3 , whereas the pulse tube cryocooler design describe here with a pressure ratio of 1.3 at the cold end (1.4 at the compressor) required a swept volume of only 0.18 cm^3 to provide a PV power of 22.2 W. That small swept volume was for an assumed cold end phase angle of -30° . A cold-end phase angle of 0° would require a significantly larger swept volume. For a swept volume of 0.18 cm^3 , an average pressure of 5.0 MPa, and a calculated pressure ratio of 1.40 at the

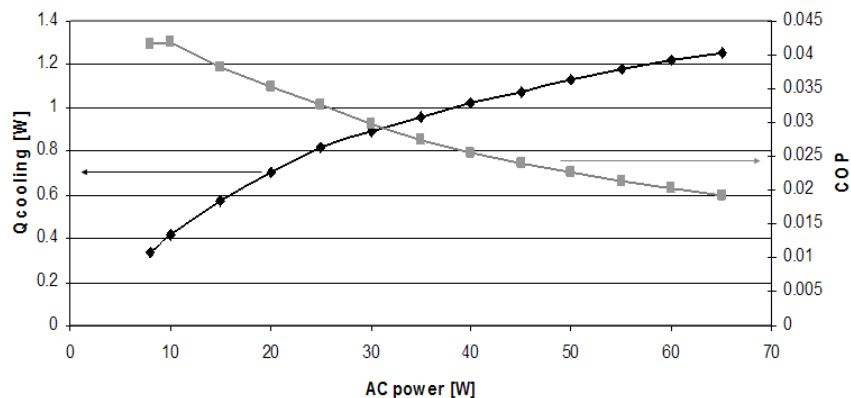


Figure 13. Net refrigeration power and COP as a function of the input electrical power at a temperature of 140 K.

Table 2. Parameters for the Ricor K527 and K529 compressors.

	K527	K529
Piston diameter, D (mm)	9.5	10
Pk-pk stroke, s (mm)	8.0	10
Swept volume, V_{co} (cm ³)	0.567	0.785
Moving mass, m (g)	30	50
Spring constant, k (N/m)	2000	0
Force constant, α (N/A)	5.0	8.0
Damping coefficient, c (N·s/m)	0-1	0-1
Coil resistance, R (Ω)	0.36	1.75
Maximum current, I_{max} (A rms)	5.0	5.0
Quality factor, $\alpha s/R$ (N·m/(A· Ω))	0.111	0.0457

compressor, the calculated force diagram for the K527 compressor is shown in Figure 15 (a small damping coefficient of 1 N·s/m was assumed). Because the motor force phasor is calculated to have a phase of 69° (with respect to the real axis) at the design operating conditions, the efficiency should be close to the maximum that occurs at resonance ($\sin 69^\circ = 0.93$). The compressor efficiency was calculated to be only 63 % at these design conditions. The required input electrical power then becomes 35.1 W with a motor current amplitude of 8.2 A or 5.8 A rms. If the pressure ratio were to be lowered to 1.26 with the same cold head flow and phase, this compressor would operate at its resonance condition and have an efficiency of 72 %. With the K529 compressor the motor force phasor was calculated to be 98° , which means that the 150 Hz operating frequency is somewhat higher than the resonance frequency. Measured values of the K529 compressor efficiency showed that it had a peak at about 135 Hz with an average pressure of 5.0 MPa.

A compressor achieves its maximum efficiency at resonance conditions, but that resonant efficiency can still be considerably less than 1.0 under certain conditions. We now examine the compressor resonant efficiency. We consider

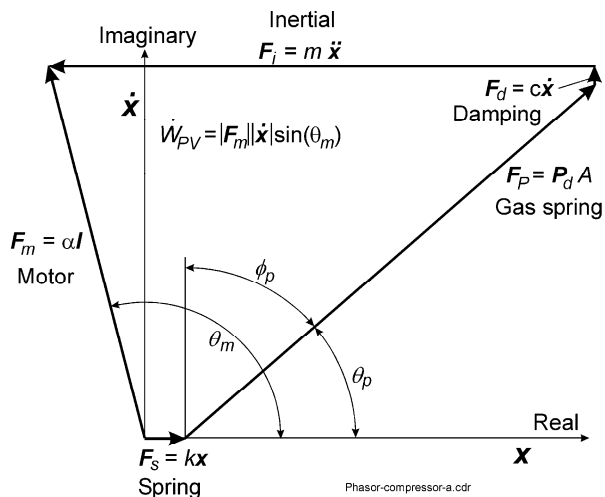


Figure 14. General force balance on a linear compressor.

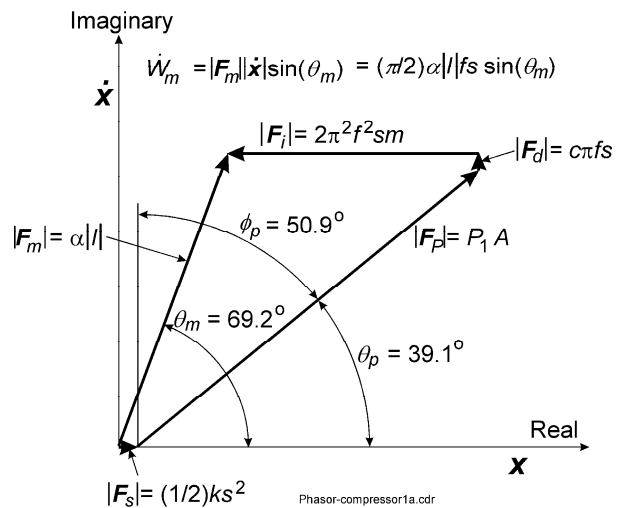


Figure 15. Force balance for K527 compressor with cold head design.

the case where eddy currents, hysteresis, and piston blowby are neglected. The compressor efficiency (or COP) is given by

$$\eta_{co} = \frac{\dot{W}_{pv}}{\dot{W}_{el}}, \quad (11)$$

where \dot{W}_{pv} is the PV power delivered by the piston, and \dot{W}_{el} is the input electrical power. The mechanical power delivered by the motor is given by

$$\dot{W}_m = \frac{1}{2} \alpha |I| f s \sin \theta_m, \quad (12)$$

where α is the force constant of the motor, $|I|$ is the current amplitude, f is the frequency, s is the peak-to-peak stroke, and θ_m is the phase of the motor force phasor. At resonance θ_m is 90° , so $\sin \theta_m = 1$. The power dissipated by the damping force is

$$\dot{W}_{damp} = \frac{1}{2} \beta \pi^2 f^2 s^2, \quad (13)$$

where β is the damping coefficient. The motor mechanical power that is available to deliver PV power can be expressed as

$$\dot{W}_{pv} = \dot{W}_m - \dot{W}_{damp} = \frac{1}{2} \alpha |I| f s - \frac{1}{2} \beta \pi^2 f^2 s^2. \quad (14)$$

The compressor resonance efficiency is then found by substituting equation (14) into equation (11), which gives

$$\eta_{co} = \frac{\frac{1}{2} \alpha |I| f s - \frac{1}{2} \beta \pi^2 f^2 s^2}{\frac{1}{2} \alpha |I| f s + \frac{1}{2} |I|^2 R}, \quad (15)$$

where R is the resistance of the coil, which gives rise to the Joule heating term in the denominator of equation (15). Equation (15) can be simplified to

$$\eta_{co} = \frac{1 - \frac{\pi \beta f s}{\alpha |I|}}{1 + \frac{|I| R}{\pi \alpha f s}}. \quad (16)$$

The ratio $(\alpha s/R)$ for a linear compressor represents a type of quality factor, where high values of the ratio lead to higher intrinsic efficiencies, as shown in equation (16). We see from equation (16) that for small values of the damping coefficient, higher frequencies lead to higher resonance efficiencies. We assume here that the moving mass is always adjusted to provide resonance for any frequency. Of course, at sufficiently high frequencies it becomes impossible to make the moving mass small enough to maintain resonance. At full stroke and at the maximum allowed operating current the resonance efficiencies are 0.881 for the K527 compressor and 0.753 for the K529 compressor at 150 Hz if a zero damping coefficient is assumed. For the design conditions of the 150 Hz miniature pulse tube cryocooler described here the full stroke was not required to provide the flow rate designed for the cold head. However, because of the high pressure amplitudes used in the cryocooler designed here, the compressor current and PV power were high. For the cold head design discussed here the ratio of required stroke to full stroke was 0.317 at a current of 5.8 A rms for the K527 compressor and 0.264 at a current of 3.59 A rms for the K529 compressor. With those parameters the compressor resonance efficiencies become 0.669 for the K527 and 0.528 for the K529, compared with 0.63 for the calculated efficiency at the off-resonance design conditions for the K527 compressor.

Figure 16 shows how the resonance efficiency of the K527 compressor varies with relative stroke at the maximum rated current of 5.0 A rms for various frequencies, assuming zero damping and at 150 Hz for the case of a damping coefficient of 1.0 N-s/m. Figure 17 shows how the resonance efficiency varies with current for operation at full stroke and with various frequencies. The results shown in Figure 16 show the importance of having the compressor operating near its full stroke to achieve high compressor efficiency. For the cold head designed here it required the K527 compressor to operate at only 31.7 % of its full stroke, which led to low compressor efficiency. In addition, the extra void volume of the large compression space contributes to irreversible heat transfer losses within this space. The high

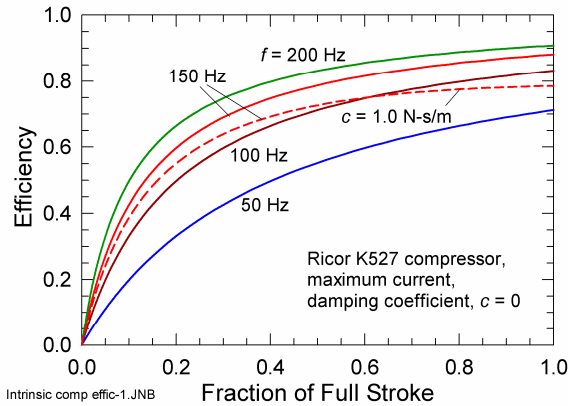


Figure 16. Efficiency of K527 compressor at resonance at the maximum rated current of 5.0 A rms.

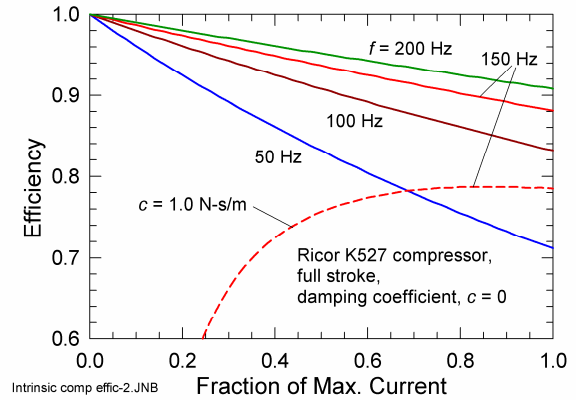


Figure 17. Efficiency of K527 compressor at resonance at full stroke.

frequency and high pressure forced the compressor to run at a current level somewhat higher than the rated maximum, which further reduced the compressor efficiency. As shown in Figure 17 the compressor efficiency decreases as current increases. The compressor efficiency can be increased by operating at lower pressure ratios. However, as shown in Figure 17 even a small damping coefficient can significantly reduce the compressor efficiency when the compressor is operated at current levels somewhat lower than the maximum allowed. A compressor with a smaller diameter piston and less swept volume would be a better match for the cold head designed here. However, in that case the moving mass would need to be significantly reduced to maintain resonance. Alternatively, the use of a smaller pressure ratio in a redesigned cold head would make the cold head match the compressor better and provide a higher overall efficiency than the present combination of cold head and compressor.

4. CONCLUSIONS

We have shown by use of models that the use of frequencies around 150 Hz should provide high power densities with high efficiencies in pulse tube cryocoolers, as long as high average pressures and small hydraulic diameters are used in the regenerator. A miniature, 150 Hz pulse tube cryocooler was designed for 1 W of cooling at 80 K. The regenerator diameter and length were only 4.5 mm and 27 mm, respectively. The designed averaged pressure of 5.0 MPa with a cold-end pressure ratio of 1.3 further contributed to the high power density. However, the experimental device only achieved a lowest temperature of 97 K due to a poor acoustic match to the small Ricor K527 and K529 compressors. The swept volume of these compressors was considerably larger than required, which led to low compressor efficiencies at the conditions required by the cold head even though the compressor operated near resonance. The low efficiency prevented the compressor from achieving a pressure ratio above 1.2 before the current significantly exceeded the current limit of each compressor. A compressor with a smaller piston diameter would be a closer match to the high power density cold head. Alternatively, the use of a lower pressure ratio in the cold head would reduce the power requirement of the compressor and keep it operating within its current limit, but the power density of the cold head would be sacrificed. This study shows the importance of matching the compressor and cold head characteristics not only for achieving compressor resonance, but also for operating near the swept volume and current limits of the compressor.

ACKNOWLEDGEMENTS

We acknowledge valuable assistance and discussions with P. Bradley, M. Lewis, and Z. Gan.

REFERENCES

1. R. B. Peterson and M. Al Hazmy, "Size limits for Stirling cycle refrigerators," *Adv. Cryogenic Engineering*, Vol. 43, pp. 997-1002, Plenum Press, New York, 1998.

2. J.M. Shire, A. Mujezinovic, and P.E. Phelan, "Investigation of microscale cryocoolers," *Cryocoolers 10*, pp. 663-670, 1999.
3. R. Radebaugh and A. O'Gallagher, "Regenerator operation at very high frequencies for microcryocoolers" *Adv. Cryogenic Engineering*, Vol. 51, pp. 1919-1928, AIP, 2006.
4. R. Radebaugh, "Microscale heat transfer at low temperatures," in *Microscale Heat Transfer -- Fundamentals and Applications*, S. Kakac ed., pp. 93-124, Springer, 2005.
5. M.E. Moran, "Microsystem cooler development" Proc. Second International Energy Conversion Conference, Providence, Rhode Island, August 16-19, 2004.
6. P. Nika and Y. Bailly, *et al*, "Miniature pulse tube for the cooling of electronic devices; functioning principles and practical modeling," *Microscale Thermophysical Engineering*, Vol. 8, pp. 301-325, 2004.
7. I. Garaway and G. Grossman, "A study of a high frequency miniature reservoirless pulse tube" *Adv. Cryogenic Engineering*, Vol. 53, pp., AIP, 2008.
8. S. Vanapalli, M. Lewis, Z. Gan, and R. Radebaugh, "120 Hz pulse tube cryocooler for fast cooldown to 50 K," *Appl. Phys. Letters*, Vol. 90, issue 7, 072504, 2007.
9. M. Petach, M. Waterman, G. Pruit, and E. Tward, "High frequency coaxial pulse tube microcooler," *Cryocoolers 15*, pp. 97-103, ICC Press, Boulder, 2009.
10. I. Garaway, Z. Gan, P. Bradley, A. Veprik, and R. Radebaugh, "Development of a miniature 150 Hz pulse tube cryocooler," *Cryocoolers 15*, pp. 105-113, ICC Press, Boulder, 2009.
11. M.A. Lewis and R. Radebaugh, "Measurement of heat conduction through bonded regenerator matrix materials," *Cryocoolers 12*, pp. 517-522, Plenum Press, New York, 2003.
12. J. Gary, D.E. Daney, and R. Radebaugh, "A computational model for a regenerator," in *Proc. Third Cryocooler Conference, NIST Special Publication 698*, pp. 199-211, 1985.
13. J. Gary and R. Radebaugh, "An improved model for the calculation of regenerator performance (REGEN 3.1)," *Proc. Fourth Interagency Meeting on Cryocoolers*, David Taylor Research Center Technical Report DTRC91/003, pp. 165-176, 1991.
14. R. Radebaugh, M. Lewis, E. Luo, J.M. Pfothenauer, G.F. Nellis, and L.A. Schunk, "Inertance tube optimization for pulse tube refrigerators," *Adv. Cryogenic Engineering*, Vol. 51, pp. 59-67, 2006.
15. E. Marquardt, R. Radebaugh, and P. Kittel, Design equations and scaling laws for linear compressors with flexure springs," *Proc. 7th International Cryocooler Conference: Air Force Report PL-CP-93-1001*, pp. 783-804, 1993.